



Effect of Aging on the Fatigue Crack Growth Behaviour of SS 316(N) Welds at Ambient Conditions

B. Shashank Dutt¹ · M. Nani Babu¹ · A. Moitra^{1,2} · G. Sasikala^{1,2} · M. Vasudevan^{1,2}

Received: 21 October 2021 / Accepted: 15 December 2021 / Published online: 28 January 2022
© Indian National Academy of Engineering 2021

Abstract

Fabrication of reactor components using SS316LN involve welding as one of the major manufacturing processes. These welds are potential sources of defects, growth of which often becomes the life-limiting factor for the components during prolonged service exposures. Many of these components are subjected to flow-induced vibrations, leading to fatigue crack initiation and growth during the operation. It calls for the evaluation of fatigue crack growth (FCG) behavior of these welds as part of ensuring the structural integrity. The FCG resistance also degrades due to aging-induced microstructural changes. The effect of aging in the temperature range 643–823 K and after 20,000 h durations on FCG properties has been evaluated at ambient temperature (298 K). The variation in the ΔK threshold with ageing has been discussed in the light of microstructural observations. The maximum benefit of ageing on FCG properties was observed at 643 K due to the crack tip branching during crack growth. Finally, the FCG data of these welds were compared with the (Design and construction rules for mechanical components for mechanical components nuclear installations (2007) RCC-MR, Section I–subsection Z: Appendix A16, (Datasheet for Austenitic Stainless Steels) pp 219. <https://www.afcen.com/en/rcc-mrx/98-rcc-mr-2007.html>) codified data and have been found to be better than that of values specified in the codes.

Keywords SS 316(N) welds · Aging · Fatigue crack growth · Fractography

Introduction

SS316LN is chosen as major structural materials for (including main vessel, intermediate heat exchanger, inner vessel, etc.) Indian nuclear reactors are based on the in house and international R&D experience. The fabrication technologies for the manufacturing of these components involve the welding process. The welded product of SS316LN is designated as SS316(N), since the carbon levels (0.04–0.05 wt%) are relatively higher than 0.03 wt% specified. Moreover, Austenitic stainless steel welds are specified to contain 5–10% delta ferrite (David et al. 1996) to avoid hot cracking (Abe and Watanabe 2008).

Generally, these welds are potential sources of defects. Maximum operating temperature for these welds is around

823 K and are subjected to flow-induced vibrations leading to high cycle fatigue. The components made by these welds are required to qualify the minimum allowable crack size and remaining life assessment. To evaluate the remaining life assessment of these welded components, it is essential to carry out the fatigue crack growth (FCG) studies in the near threshold and Paris regimes, respectively. Extensive FCG studies have been carried out on the base material as a function of nitrogen variant (Babu et al. 2019) and as received welds (Babu et al. 2010) at different temperatures. During service, these components may undergo ageing. Therefore, the effect of ageing duration and ageing temperatures on the FCG behavior has been examined. The FCG properties have been interpreted by microstructural examinations.

Experimental

The SS 316LN plate or base material was supplied having 30 mm thickness and in solution annealed condition. From the base plate, weld pads were prepared by shielded metal arc welding process. The weld pads were subjected to

✉ B. Shashank Dutt
shashank@igcar.gov.in

¹ Metallurgy and Materials Group, IGCAR, Kalpakkam, Tamil Nadu 603102, India

² Homi Bhabha National Institute, Kalpakkam, India

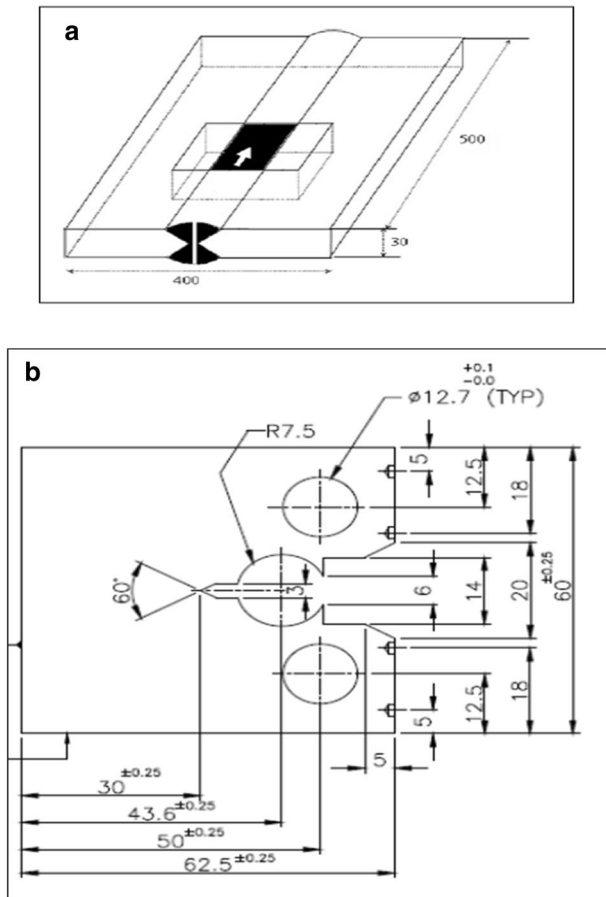


Fig. 1 CT sample drawing along with weld orientation

X-ray radiographic inspection to ensure defect-free welds. The weld pads had dimensions 500 mm length and 400 mm width. From these weld pads, specimen blanks of dimensions 70×65×30 mm were cut and subjected to aging at 643, 748 and 823 K and for 20,000 h duration. From the as welded and aged blanks, specimens were cut and subjected to polishing and chemical etching for observation of microstructures. The aged weld blanks (including un-aged condition) were further fabricated into compact tension (CT) specimens and having 20 mm thickness. The CT specimens had a width of 50 mm and a length of 62.5 mm. The drawing of CT specimen is shown in Fig. 1. The CT specimens were subjected to pre-cracking before fatigue crack growth (FCG) testing. The pre-cracking was done under cyclic loading and after pre-cracking initial crack length was targeted in the range 22.5–22.7 mm. The FCG tests were conducted at ambient (298 K) temperature and as per ASTM E 647 (ASTM 2015). The FCG tests were carried out under a frequency of 15 Hz and the load ratio (R) applied was 0.1. The FCG testing was carried out by applying ΔK values under decreasing loading conditions. The crack lengths were monitored using a suitably calibrated direct current potential drop

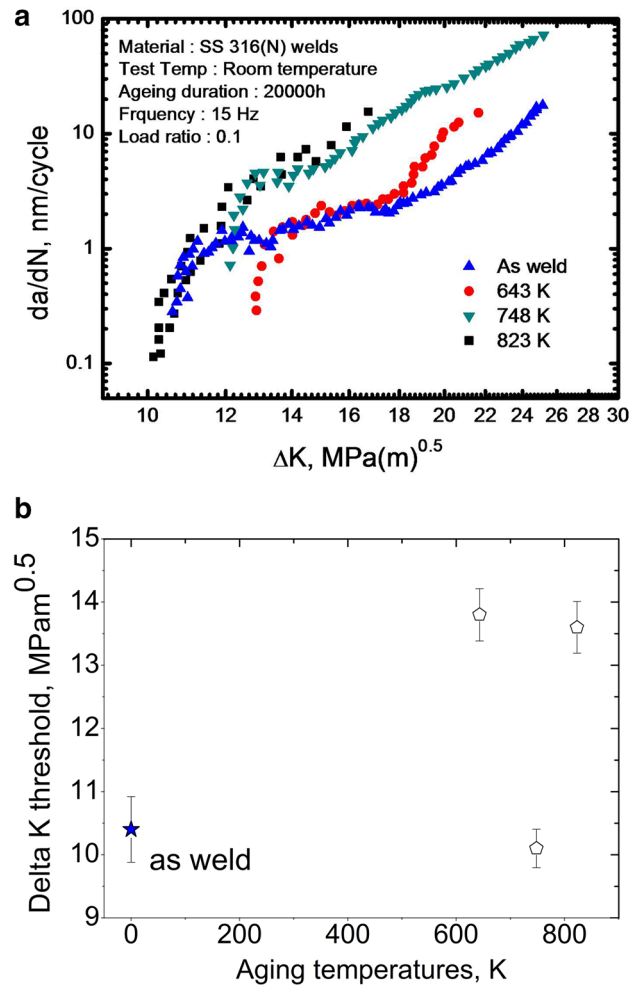


Fig. 2 a FCG results of welds after aging including as weld condition. b Delta K threshold values of welds

technique. For smoothing of FCG test results, data reduction scheme has been adopted as per ASTM E 647. After FCG testing the broken CT specimens were observed under SEM for fractographic characterization. The ΔK threshold values were determined as per ASTM E 647 for all tested specimens. For determination of ΔK threshold value, linear average of 5 uniformly spaced data points of crack growth (da/dN values) in the range 10^{-9} and 10^{-10} m/cycle were considered.

Results and Discussion

Figure 2a represents FCG data of SS316(N) welds aged at different aging temperatures. From Fig. 2a it can be observed that the slopes of FCG curves are higher after aging compared to as weld condition. The higher slopes after aging indicated better resistance to FCG, compared to without aging. The ΔK threshold value for as weld condition

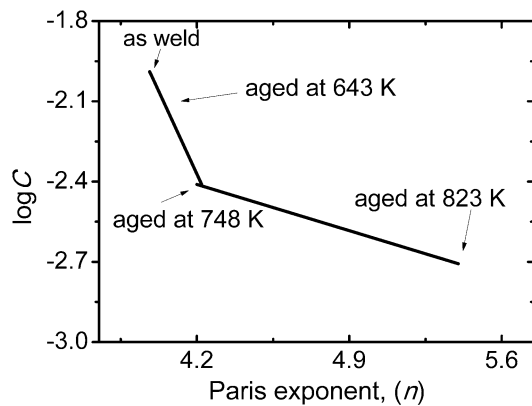


Fig. 3 Paris constant ($\log C$) and Paris exponent (n) values of welds after aging

was $\sim 10.4 \text{ MPa}\cdot\text{m}^{0.5}$. The ΔK threshold values after aging are plotted in Fig. 2b. The ΔK threshold results after aging at 643 and 823 K were higher compared to as weld condition. The maximum ΔK threshold value was observed for aging at 643 K when compared to the other ageing conditions. In the threshold regime, it is expected that increase in resistance to FCG after aging due to changes in microstructure (formation of brittle type of precipitates) and the resultant benefit in this regime. The changes in microstructure after aging are discussed in subsequent paragraphs in order to corroborate with the FCG properties observed (Figs. 2, 3). It is widely reported that in the Paris regime, driving force for crack growth is dependent on applied force K_{\max} rather than the ΔK . It is also known that crack growth occurs to a greater extent when the crack tip experiences the maximum stress (Babu et al. 2019). Improved resistance to FCG was also previously observed (Raske and Cheng 1977) for SS 308 welds after aging at 866 K for 1000 h. In the previous study (Raske and Cheng 1977) better resistance (after aging) to FCG was observed at higher levels of ΔK values (greater than $22 \text{ MPa}\cdot\text{m}^{0.5}$). In this study (Fig. 2a) also similar trends are observed (after aging) at ΔK values greater than $20 \text{ MPa}\cdot\text{m}^{0.5}$.

The Paris constants ($\log C$) and exponent (n) values are plotted in Fig. 3. After aging at 643, 748 and 823 K, increase in Paris exponent was observed compared to as weld condition. It is expected that n and $\log C$ values follow a linear trend at different aging temperatures. However, from Fig. 3, it can be observed that $\log C$ and n values follow bilinear trend. It is expected that this deviation is due to changes in the microstructure with aging. In a previous study (Babu et al. 2010) by some of the authors, Paris constant and exponent values were reported for as weld condition and at test temperatures of 300, 573 and 823 K. These constants (Babu et al. 2010) varied in a non-monotonic trend with test temperatures. In this study, it is observed

that there are two slopes in Fig. 3, indicating two different crack growth mechanisms controlling the crack growth rate. From previous studies (Vitek et al. 1991; Dutt et al. 2011) it is observed that below 748 K, embrittlement is associated with the spinodal decomposition. At 823 K, carbide precipitation is expected to occur. Thus, we can link the two slope behavior to the two operating mechanisms and one of the mechanisms is spinodal decomposition (formation of α phases within delta ferrite). It has been observed (Vitek et al. 1991) that partial spinodal decomposition resulted in modulated structure. It is also expected that during crack growth interaction of this kind of modulated structure can lead to crack branching thereby enhancing the crack growth resistance under cyclic load. However, earlier studies (Dutt et al. 2018) showed decrease in fracture resistance due to the changes in microstructure. Thus, it can be worth noted that these changes in microstructure resulted in beneficial effects towards resistance to crack growth under cyclic loading.

To support the observation of the FCG properties, microstructure characterization has been carried out for all the tested specimens before and after the ageing. Figure 4 (a through d) shows the optical images of as-weld, aged at 643, 748 and 823 K for 20,000 h. The microstructures revealed austenite matrix and delta ferrite with vermicular morphology. Similar results of optical microstructures were previously (Vitek et al. 1991) reported for SS 308 welds. In this study, the extent of this morphology changes with ageing temperatures are observed in Fig. 4a–d. The different kinds of interpenetrating shape and location of δ -ferrite may play a significant role on the crack growth resistance during the crack growth under cyclic loading. In addition to the morphology of delta ferrite, phase boundary and its orientation can contribute to crack growth resistance. After aging at 748 (Fig. 4c) and 823 K (Fig. 4d), the morphology of delta ferrite network was changed at a few regions of the microstructure. It is also to be noted from Fig. 4c (aged at 748 K) that at a few delta ferrite regions were relatively coarser. Such coarser were also observed at different locations of specimens for other aging conditions also. It was also observed that after aging for these three aging temperatures, only at limited locations of specimens delta ferrite was coarser. It is expected that at 643 and 748 K, formation of α phase (within delta ferrite by spinodal decomposition) occurred, as reported previously (Vitek et al. 1991). At 823 K (Fig. 5a) formation of carbide-based precipitate was observed as revealed by EDX results of the precipitate, shown in Fig. 5b. Some of the authors have previously mentioned no significant changes in tensile properties of these welds after aging at similar aging conditions (Dutt et al. 2018). The crack path deviations during FCG were observed as shown in Fig. 6a–d. It is expected that a higher extent of crack path tortuosity

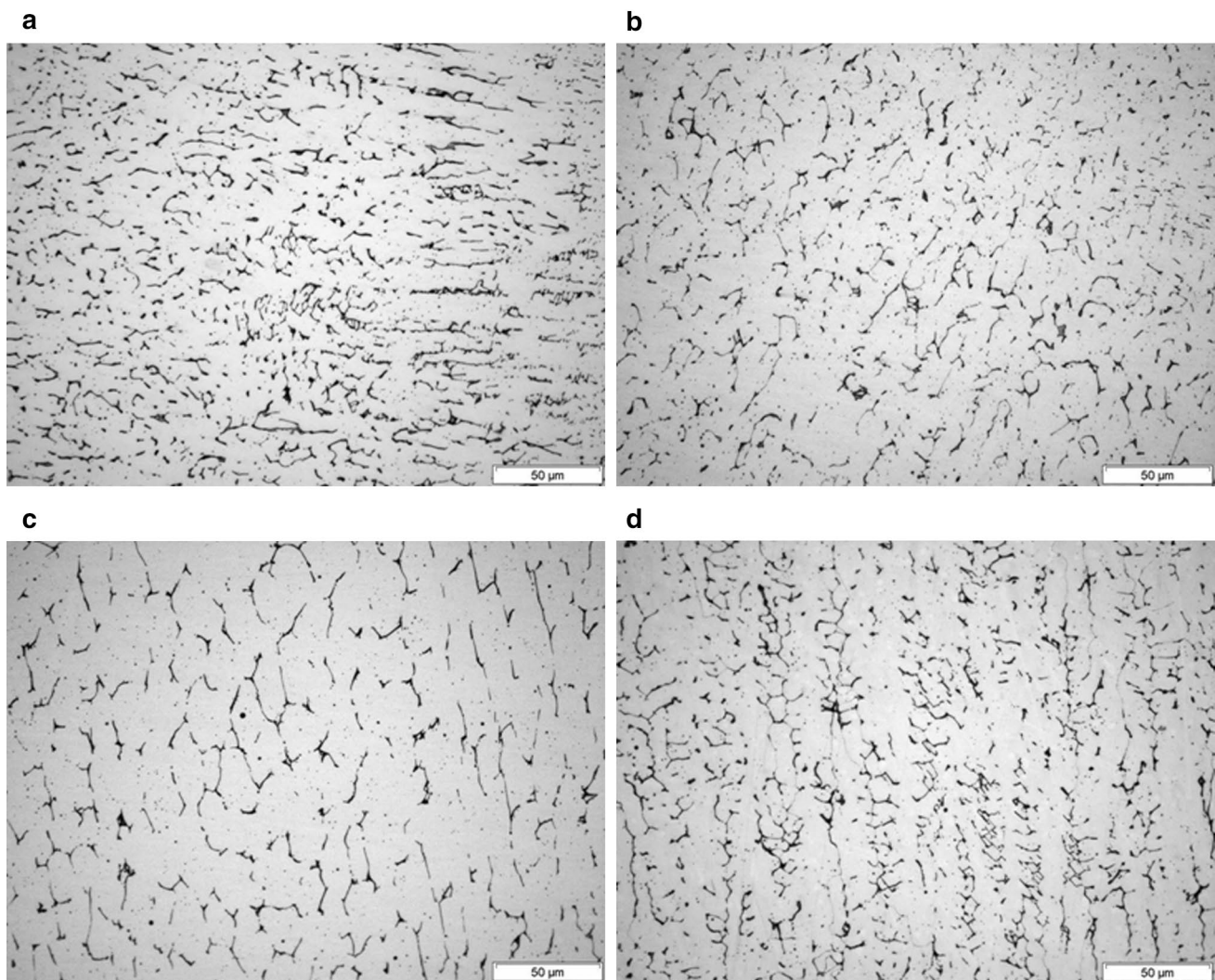


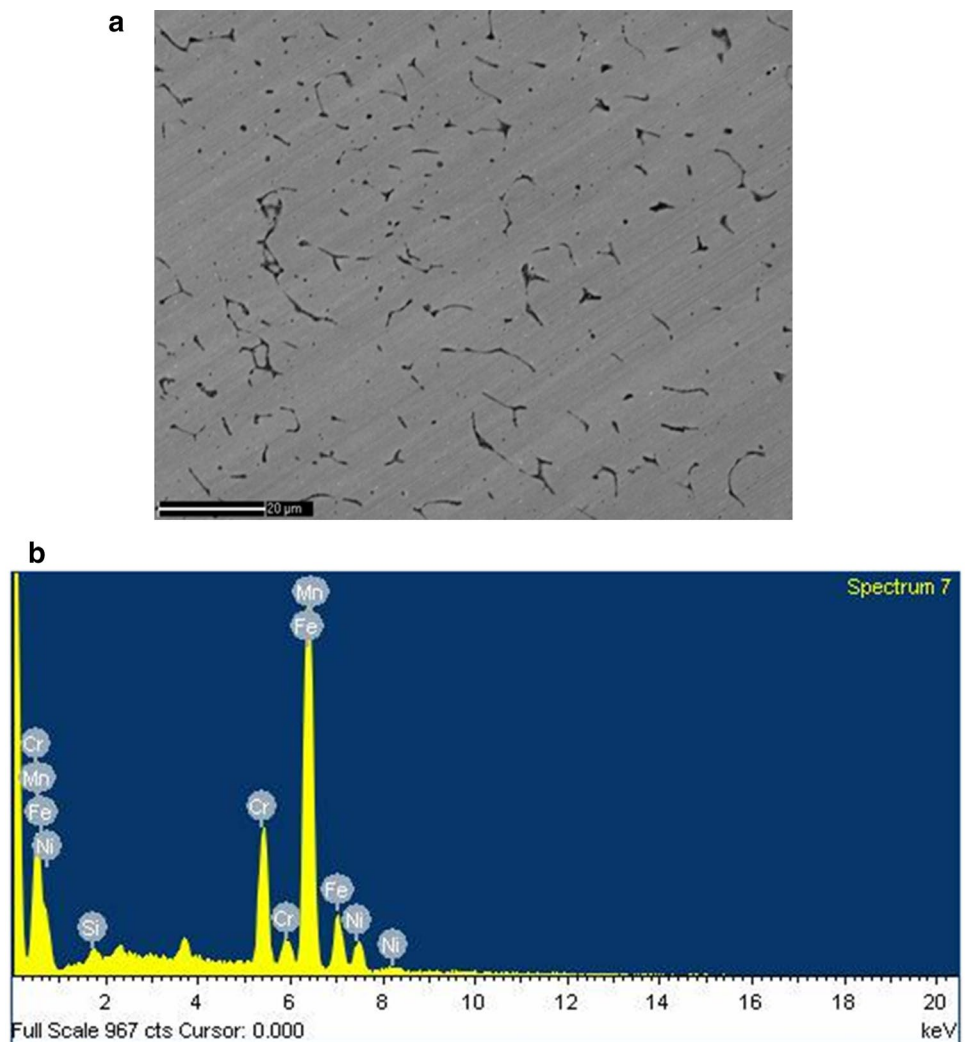
Fig. 4 a–d optical microstructures of SS 316(N) welds after aging **a** as weld condition, **b** aged at 643 K, **c** aged at 748 K and **d** aged at 823 K

results in better fatigue crack growth resistance. In a weld condition, the presence of delta ferrite acting as a hindrance to crack growth was previously reported (Babu et al. 2010). Increase in FCG resistance with aging can be correlated to the presence of precipitates. These precipitates act as a hindrance to crack growth (James 1974). The extent of crack path deviations was higher after aging at 643 K (Fig. 6b) and 748 K (Fig. 6c) compared to 823 K (Fig. 6d). The relatively higher ΔK threshold values at 643 K and 748 K, compared to 823 K are in line with the observed crack path deviations.

Figure 6a revealed crack path deviation for as weld condition. After aging at 643 K, crack deviation and crack branching was observed (Fig. 6b). The conjoint influence of crack

path deviation and crack branching may contribute to higher crack growth resistance by reducing the crack growth driving force into mode I and mode II. At other aging conditions (748 and 823 K) negligible extent of either crack path deviation or crack branching was observed as revealed in Fig. 6c–d. Thus, it is anticipated that the FCG resistance is better near threshold for aged material at 643 K. These observations are in consistent with the earlier studies (Babu et al. 2010). Similar improvements in resistance to FCG were previously reported for SS 304 welds (James 1974) after aging at 538 °C (1500 h) and tested at 538 °C. Increase in resistance to FCG can be correlated with the role of precipitates and second phase particles acting as arrestors for

Fig. 5 a, b Microstructure of SS 316(N) welds after aging at 823 K **(b)** EDX result of carbide precipitate



crack propagation (James 1974). However, at Paris regime crack growth occurs predominantly by crack tip blunting and re-sharpening mechanisms. During this process, δ -ferrite is likely to promote crack tip blunting and the presence of carbide precipitates could lead to re-sharpening of crack. However, it is observed (Fig. 2a) that the overall FCG resistance decreases with the ageing temperature because the order of magnitude of crack tip opening displacement is usually observed to be much higher than the ferrite thickness ($\sim 3\text{--}5\ \mu\text{m}$) and precipitate size ($\sim 90\text{--}100\ \text{nm}$). The fractographic examinations are shown in Fig. 7a–d.

It can be observed from Fig. 7a–d that crack propagation was predominantly by transgranular mode. From Fig. 7b and c it can also be observed that the fracture surface was predominantly more coarser at 643 and 748 K, compared to 823 K

(Fig. 7d). These fractographic observations are in line with better resistance to FCG observed at 643 and 748 K (Fig. 2a) compared to 823 K. Fractographic (Fig. 7d) examination at 823 K revealed the presence of few carbide precipitates. Some of these carbide particles are located in different regions nearby to various striations (Fig. 7d) formed during the crack growth process.

The FCG results in this investigation are compared to previous design guidelines (RCC-MR 2007). The delta K threshold values in the temperature range 20–650 °C for this class of welds was reported by Eq. 1.

$$\Delta K_{\text{threshold}} = 6.5 - 4.5R \quad (1)$$

where R is the applied load ratio. In this study R value was 0.1 and delta K threshold estimated from Eq. (1)

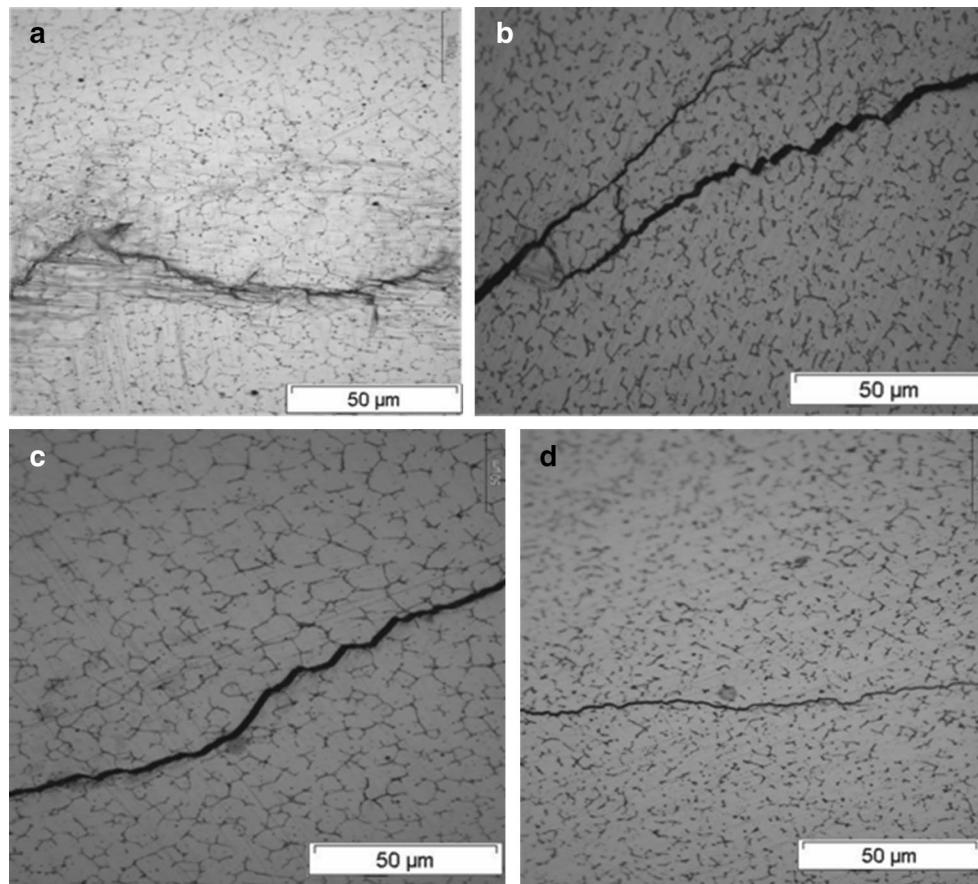


Fig. 6 a–d Optical micrographs showing crack path deviations and crack branching for **a** as welded **b** aged at 748 K and **c** Aged at 823 K and **d** aged at 823 K

was $\sim 6 \text{ MPam}^{0.5}$. In this study, experimentally determined delta K threshold values were in the range $10\text{--}13 \text{ MPam}^{0.5}$ and these values are higher than those previously specified in design guidelines (RCC-MR 2007).

Conclusions

1. A moderate increase in delta K threshold value ($\sim 13.6 \text{ MPam}^{0.5}$) was observed after aging at 643 K compared to as weld ($10.4 \text{ MPam}^{0.5}$) condition.
2. Increase in Paris exponents in the range (4.1–5.4) was observed after aging at 643, 748 and 823 K, compared to as weld condition (n value of ~ 4.0).
3. Increase in resistance to FCG after aging at 643 K can be explained based on hardening of matrix due to spinodal decomposition. The extent of crack path tortuosity and crack branching was higher after this aging condition.
4. After aging at 823 K, a moderate decrease in FCG resistance observed was predominantly due to carbide precipitation.

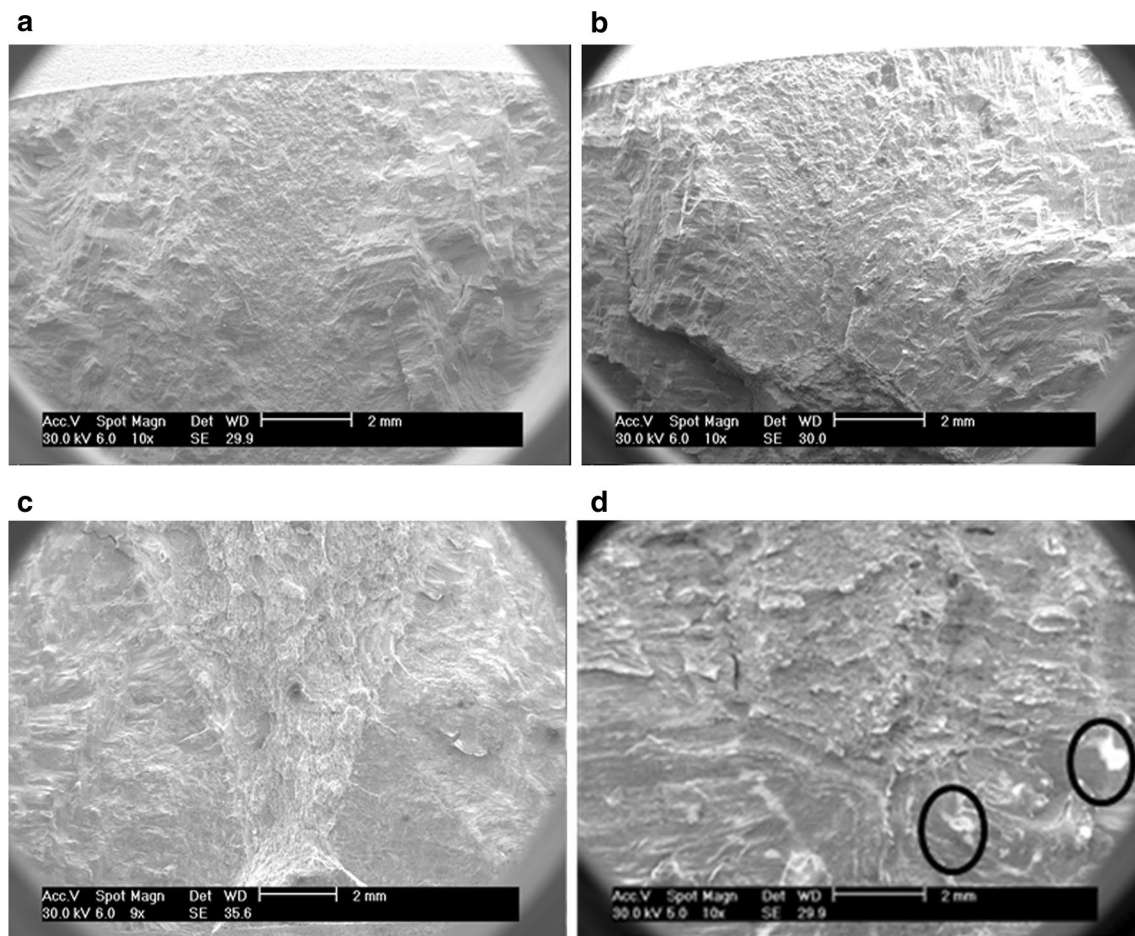


Fig. 7 a–d Fractographs of SS 316(N) welds **a** as weld condition and after aging at **b** 643 K **c** 748 K and **d** 823 K

References

- Abe H, Watanabe Y (2008) Low-temperature characteristics of type 316L stainless steel welds: dependence on solidification mode. *Metall Mater Trans A* 39:1392–1398. <https://doi.org/10.1007/s11661-008-9511-8>
- ASTM E647–15e1 (2015) Standard Test Method for Measurement of Fatigue Crack Growth Rates, ASTM International, West Conshohocken, PA <https://www.astm.org>
- Babu MN, Dutt BS, Venugopal S, Sasikala G, Bhaduri AK, Jayakumar T, Raj B (2010) On the anomalous temperature dependency of fatigue crack growth of SS 316 (N) weld near threshold. *Mater Sci Eng A* 527:5122–5129
- Babu MN, Sasikala G, Sadananda K (2019) Effect of nitrogen on the fatigue crack growth behavior of 316L austenitic stainless steels. *Met Trans* 50:3091–3105. <https://doi.org/10.1007/s11661-019-05225-w>
- David SA, Vitek JM, Alexander DJ (1996) Embrittlement of austenitic stainless steel welds. *J Nondestruct Eval* 15:129–136. <https://doi.org/10.1007/BF00732040>
- Dutt BS, Sasikala G, Shanthi G, Venugopal S, Babu MN, Parida PK, Bhaduri AK (2011) Mechanical behaviour of SS 316 (N) weld after long term exposure to service temperatures. *Procedia Eng* 10:2725–2730
- Dutt BS, Babu MN, Shanthi G, Moitra A, Sasikala G (2018) Effect of thermal aging and test temperatures on fracture toughness of SS 316(N) Welds. *J Mater Eng Perform* 27:6577–6584. <https://doi.org/10.1007/s11665-018-3255-4>
- James LA (1974) Effect of thermal aging upon the fatigue-crack propagation of austenitic stainless steels. *Met Trans* 5:831–838. <https://doi.org/10.1007/BF02643135>
- Raske DT, Cheng CF (1977) Fatigue crack propagation in types 304 and 308 stainless steel at elevated temperatures. *Nuclear Technol* 34:101–110. <https://doi.org/10.13182/NT77-A31834>
- RCC-MR (2007) Design and construction rules for mechanical components for mechanical components nuclear installations, RCC-MR, Section I–subsection Z: Appendix A16, (Data sheet for Austenitic Stainless Steels) pp 219. <https://www.afcen.com/en/rcc-mrx/98-rcc-mr-2007.html>
- Vitek JM, David SA, Alexander DJ, Keiser JR, Nanstad RK (1991) Low temperature behavior of type 308 stainless steel weld metal. *Acta Metall* 39:503–516

Publisher's Note Springer Nature remains neutral with regard to jurisdictional claims in published maps and institutional affiliations.